River Flow 2010 - Dittrich, Koll, Aberle & Geisenhainer (eds) - © 2010 Bundesanstalt für Wasserbau ISBN 978-3-939230-00-7

Flash flood simulation of the Toga River caused by localized torrential rain in urbanized area

I. Fujita
Department of Civil Engineering,Ggraduate School of Engineering, Kobe University, 1-1 Rokkodai-cho, Nada-ku,Kobe, 657-8501, Japan

Y. Kunita
Graduate student, Department of Civil Engineering, Ggraduate School of Engineering, Kobe University, 1-1 Rokkodai-cho,Nada-ku, Kobe, 657-8501,Japan

ABSTRACT: In the afternoon of July 28 in 2008, a flash flood occurred suddenly in water-friendly reach of the Toga River in Kobe City and tragically, five people were drowned by the flood. They were among about fifty people enjoying the river environment at the site. The flash flood was caused by a sudden localized torrential rain in the urbanized area of the river basin. Noteworthy fact with this flood is the flow image was successfully captured by a river monitoring camera installed by the local government and it was made clear that the sudden water rise occurred at least within two minutes, indicating that the flood entering the accident site was like a tsunami flowing down the river. The flow was almost supercritical and water level rose locally by transverse steps installed in a steep bed slope of about 1/20. In order to investigate the flow feature more in detail, we conducted a two-dimensional flow simulation using laser-scanned data as bathymetry information, from which distribution of hydrodynamic force acting on the people in the river was estimated, demonstrating the difficulty of evacuation in flash flood condition even when the water depth is lower than the knee level.

Keywords: Flash flood, Water accident, 2D-simulation, Evacuation, Hydrodynamic force, Water-friendly environment

1 INTRODUCTION

The Toga River is one of the twenty four small-scale second-class rivers in Kobe City flowing down southward to the Seto Inland Sea from the Rokko Mountains. Toga River has been famous for enthusiastic activities by the local people aiming at recovering water-friendly river environment from the worst condition with dirty trash during the high-growth era about thirty years ago. With their persistent efforts and the financial support by the city government, the river environment as well as river structure has been improved significantly in recent years even though the river is located in the center of a big city, for example freshwater fish such as sweetfish has come to be inhabitable by installing well-designed fish ladders. This attracts more people to the Toga River than the other rivers in Kobe City.

However, in the afternoon of July 28 in 2008 a flash flood suddenly occurred due to a torrential rain accompanying cumulonimbus clouds and it resulted in a tragic accident killing human lives. It should be noted that different from loss of life caused by large-scale flash flood (Dekay and McClelland, 2006, Jonkman, et al., 2002), the present accident occurred in an extremely small scale river basin which had attracted local people. In order to investigate the cause of the water accident, we try to reproduce the flow situation by a two-dimensional simulation model as much as possible and calculate the distribution of hydrodynamic force acting on the people in the river.

2 OUTLINE OF THE WATER ACCIDENT

2.1 *Toga River*

The main reach of the Toga River is located in Kobe City with two small tributary streams, the Rokko River and the Somatani River, as indicated in Figure 1. The length of the main river is 1.79km and the drainage area is 8.57 km^2, which is roughly a common scale of the rivers flowing in Kobe City. One of the outstanding features of the Toga River is its bed slope; the slope is 1/200 even at the river mouth and more than 1/20 at the

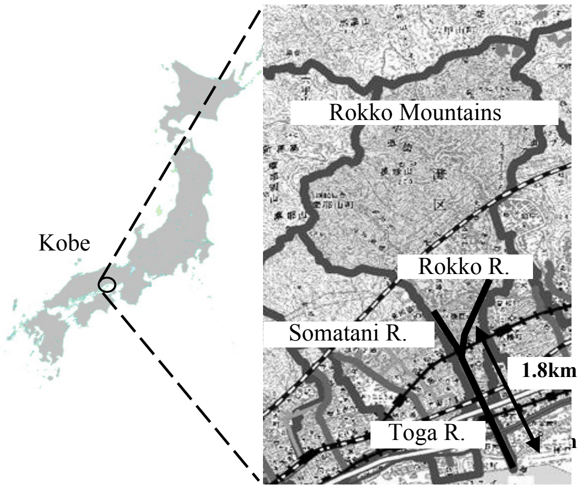

Figure 1. Toga River Basin

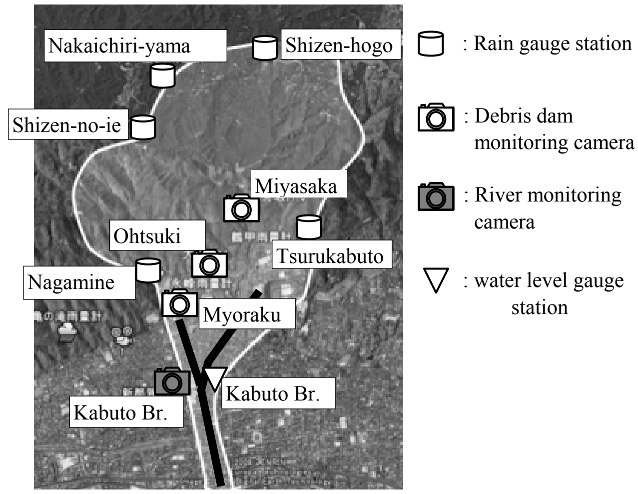

Figure 3. River monitoring systems

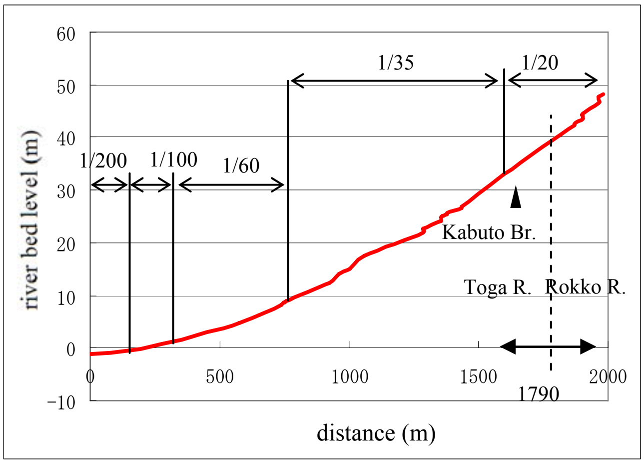

Figure 2. River bed profile

upstream end of the main river as shown in Figure 2. The channel cross section is trapezoid with a bottom width of about fifteen meters at most of the sections. The side walls and the bottom is fixed by concrete, however, small meandering lower stream with efficient fish ladder is installed in the center of the channel. In addition, side stairs are installed at many locations for improving the accessibility to the riverfront. The lower river basin is mostly occupied by residential houses and paved streets developed up to the foot of the mountainous area. Therefore, a storm drainage system is installed for preventing inland flood. Most of the inland water is conveyed to the main river through pipes or ducts.

2.2 *Arrangement of monitoring systems*

A remarkable feature regarding the Toga River basin is that a variety of monitoring systems are installed within the area, which were eventually quite useful in revealing the characteristics of the flash flood to be described later. The available systems are a) five rain gauge stations, b) a water gauge station, c) a river monitoring camera, and d) three debris dam monitoring cameras. Figure 3 shows the location of the respective stations. The rain and water gauges collect data every ten minutes, while the river monitoring camera installed at the Kabuto Bridge captures a still image every two minutes. On the other hand, the debris dam cameras intend to record video images of the flow over the dam crest. In addition to the above monitoring systems, the Japan Meteorological Agency provides rainfall information with a resolution of 1 km by 1 km measured by a weather radar system every ten minutes.

2.3 *Hydrological and hydraulic data*

Hyetographs at each rain gauge station are provided in Figure 4. It is obvious that rainfall intensity is stronger in *the* downstream urban area than in the upstream forest area. Surprisingly, at the Tsurukabuto station, the rainfall increases suddenly up to 24mm per ten minutes from almost no rain condition. The rainfall continued for about an hour, rapidly decreasing its intensity after the peak.

According to the water level hydrograph shown in Figure 5, the water level at the Kabuto station rose 1.34m in ten minutes. The peak water level condition continued for about ten minutes followed by gradual decrease of water depth. The water depth before the flash flood is about ten centimeters, which is a normal flow condition of this river.

2.4 *Monitoring camera capturing water accident*

The river monitoring camera installed downstream of the Kabuto Bridge successfully captured what had happened during the flash flood. Figure 6 displays several consecutive images before and after the flash flood. Figure 6(a) is the image twenty minutes before the arrival of the flash flood. As can be observed, there are several people including children enjoying the river. It has been re-

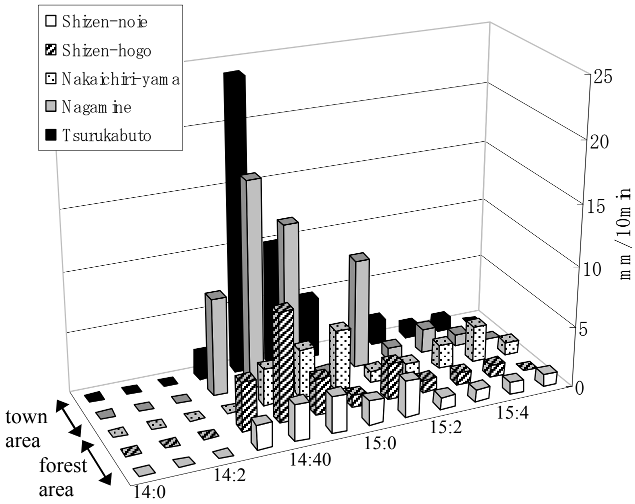

Figure 4. Hyetographs at rain gauge stations

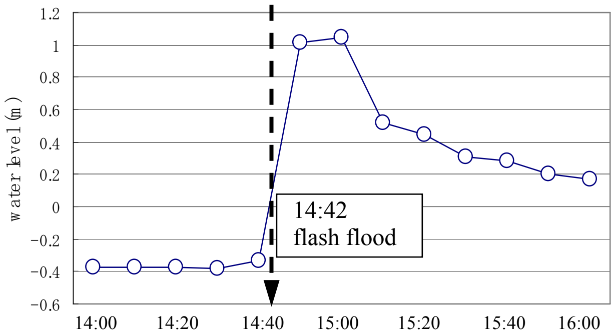

Figure 5. Water level hydrograph at Kabuto Bridge

(a) 20 min before flash flood

(d) 2 min after arrival

(b) 10 min before flash flood

(e) 10 min after arrival

(c) flash flood just arrived

(f) 20 min after arrival

Figure 6. River monitoring images before and after arrival of flash flood

ported that more than fifty people were playing in the river at the time. The weather is fine with no rain. Actually, the weather in this area had been fine for a month before the flash flood occurred. The rain caused by the development of cumulonimbus clouds started ten minutes before the event. Figure 6(b) is the image ten minutes before the flash flood, at which time the torrential rain began to fall and people within the image have evacuated from the river. However, there were still many people left in the river downstream of the section. Figure 6(c) shows the image just when the flash flood arrived at the site. It is apparent that the water depth increases significantly with large water surface undulation. The side walking ways are also covered with water. It has to be mentioned from these images that the sudden increase of water depth occurred almost within two minutes and not in ten minutes as indicated in Figure 5 in terms of the water level hydrograph. This discrepancy is attributed to the fact that the water level information is transmitted to the local government office via a telemeter after averaging ten minutes of data. This flow situation continues for more than twenty minutes as can be seen from Figure 6(e) and Figure 6(f).

Unfortunately, as mentioned above, there are people who failed to evacuate from the river due to the sudden increase of water depth. Among them ten people were rescued by local residents but five people including three children were drowned to death. According to eyewitnesses of the accident, the flash flood arrived at the site just like a water wall of tsunami coming from upstream. The height of the water volume is allegedly at least more than one meter and this information is consistent with the gauging data. In fact, according to the local residents the Toga River had been known to become dangerous once a thunder storm comes to the area and actually a similar flash flood occurred in 1998 with no loss of life at that time.

3 CAUSE OF THE FLASH FLOOD

3.1 *Water catchment area*

As has already been shown in Figure 4, the rain distribution is concentrated on the urbanized town area rather than the forest area. The inflow from the forest area was examined by debris dam monitoring cameras. Figure 7 is an image of the Ohtsuki camera installed just upstream of the urban area at the time of the peak rainfall. It is obvious there occurs no inflow from the forest area through this dam, i.e. even a water surface cannot be detected from the image. This condition continues even after the peak rainfall. Since the other two cameras provided similar surface situations as well, we can conclude that the water catchment area contributing to the present flash flood is restricted only to the urbanized residential area with little influence from the rainfall in the forest area. From this information, we made a rough estimate of the peak discharge from the rational formula using the residential area, peak rainfall intensity and the runoff coefficient assumed to be unity. The calculated result, about $40m^3/s$, will be examined in the 2D simulation in the following chapter.

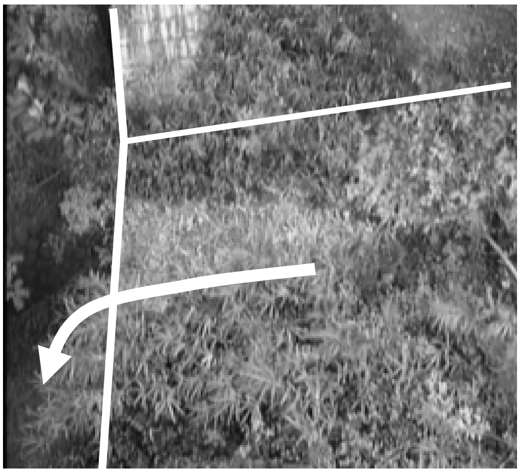

Figure 7. Image of debris dam monitoring camera at Ohtsuki

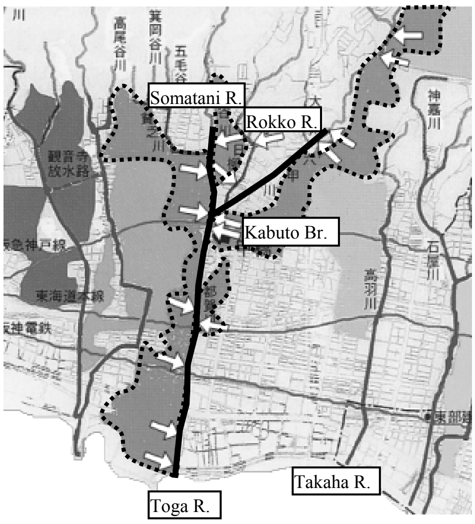

Figure 8. Stormwater drainage system of the Toga River

Figure 9. Measurement data by ground laser instrument

3.2 *Stormwater drainage system*

The residential area has a stormwater drainage system in addition to small-scale tributary channels as illustrated in Figure 8. The shadowed area bounded by dotted line corresponds to the drained area of the system. The drained water enters the major river channels through ducts or pipes at seventeen exits indicated by arrows in Figure 8, out of which twelve exits are located upstream of the Kabuto Bridge. It has been reported that the stormwater inflow to the river is extremely high like a jet at the exit. This indicates that the installed stormwater drainage system rapidly accumulated the stormwater and drained the water to the nearest river quite efficiently. This is however one of the causes of the present flash flood. The problem was there were people still left within the water course.

4 NUMERICAL SIMULATION

4.1 *Detailed bathymetry measurement*

In order to simulate the complicated flash flood features evidenced by the river monitoring camera previously demonstrated in Figure 6, it is necessary to obtain detailed bathymetry information, basically composed of walkways, fish ways and stepping stones. For this purpose, we used a ground laser instrument capable to measure the 3D ground data with a spatial resolution of several centimeters. Data for submerged river bed difficult to measure with this instrument are replaced by the manually measured values. With this procedure, a detailed bathymetry data of 1.8km of the Toga River are obtained. An example of the measurement data is indicated in Figure 9. The dots corresponding to the respective measured data represent the bathymetry information quite precisely.

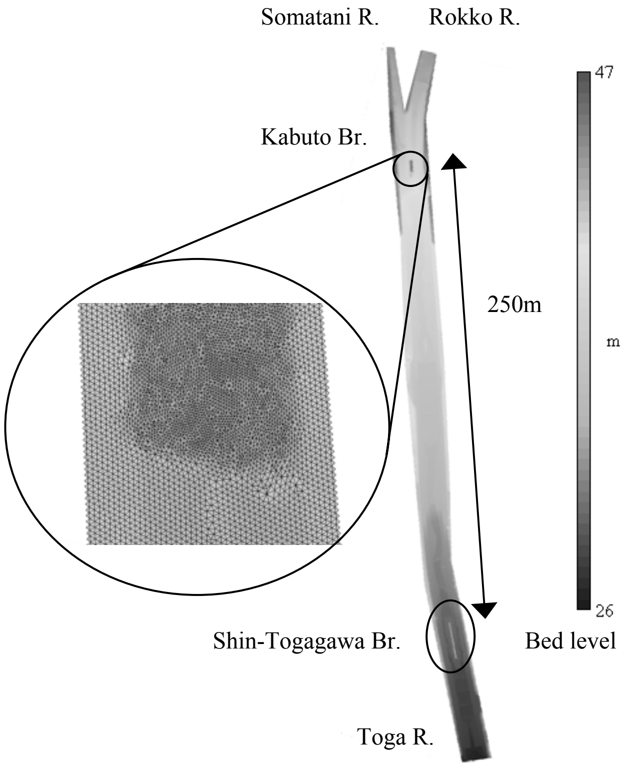

Figure 10. Range of simulation and grid arrangement

4.2 *Simulation model based on unstructured grid system*

Since it is impossible to use all of the measured bathymetry data in the simulation, the data is rearranged into a set of triangular unstructured grid. The maximum size of the grid is set at 0.6m since the size of the cubic stepping stone is about 0.6m. Smaller grid size is used near the bridge pier as shown in Figure 10. The total number of grid is about 80000 in the present simulation. The simulation model used is based on the two-dimensional shallow water equations with turbulence terms as follows:

$$\frac{\partial U}{\partial t}+\frac{\partial E}{\partial x}+\frac{\partial F}{\partial y}+S+\nu\left(\frac{\partial}{\partial x}h\frac{\partial G}{\partial x}+\frac{\partial}{\partial y}h\frac{\partial G}{\partial y}\right)+\frac{\partial H}{\partial x}+\frac{\partial I}{\partial y}=0 \quad (1)$$

where

$$U=\begin{bmatrix} h \\ uh \\ vh \end{bmatrix}, E=\begin{bmatrix} uh \\ u^2h+\frac{1}{2}gh^2 \\ uvh \end{bmatrix}, F=\begin{bmatrix} vh \\ uvh \\ v^2h+\frac{1}{2}gh^2 \end{bmatrix},$$

$$S=\begin{bmatrix} 0 \\ -gh\left(S_{0x}-S_{fx}\right) \\ -gh\left(S_{0y}-S_{fy}\right) \end{bmatrix}, G=\begin{bmatrix} 0 \\ u \\ v \end{bmatrix}, H=\begin{bmatrix} 0 \\ -\overline{u'^2} \\ -\overline{u'v'} \end{bmatrix}, I=\begin{bmatrix} 0 \\ -\overline{u'v'} \\ -\overline{v'^2} \end{bmatrix},$$

h=water depth, u=velocity in x-direction, v= velocity in y-direction, g=gravitational acceleration, ν=kinematic viscosity, S_{0x}=bed slope in x-direction, S_{0y}=bed slope in y-direction, S_{fx}=friction

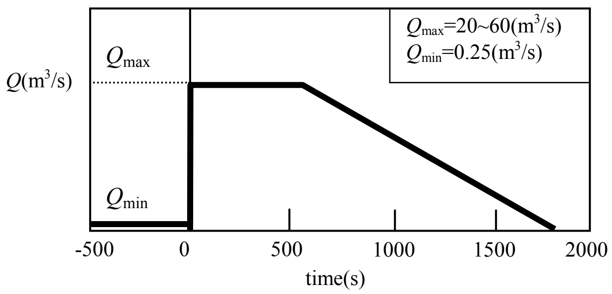

Figure 11. Input hydrograph

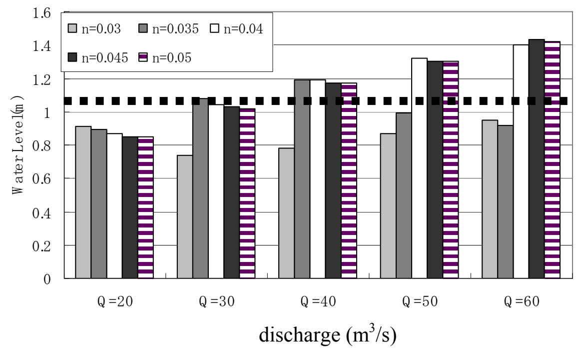

Figure 12. Comparison of water level at Kabuto Br.

slope in x-direction, S_{fy}=friction slope in y-direction, and the terms in H and I represents Reynolds stresses. The Reynolds stresses are expressed by the Boussinesq approximation.

The above equations are discretized by a finite volume method using the flux difference scheme (FDS) for the solution of the equations (Fujita and Tsubaki, 2003, Hoffman and Chiang, 1993). Initially, small discharge Q_{min}, 0.25 cubic meters per second, is applied at the upstream tributary channels until the flow becomes stable. Then, a sudden increase of flow with a peak discharge of Q_{max} is supplied to simulate the flash flood as shown in Figure 11. The input discharge is divided in half and supplied at the upstream two tributary channels. The effect of the respective drainage channels were not taken into account in the present simulation.

4.3 *Estimation of hydraulic parameters*

The simulation is performed by varying the value of Q_{max} between 20m^3/s and 60m^3/s and the Manning's roughness coefficient between 0.03 and 0.05 to find the most appropriate combination of the parameter representing the actual flow situation. The tuning conditions of the parameters are as follows:

(a) the water depth at the gauging station upstream of the Kabuto Br.

(b) the water depth on the side walkways estimated by images of the monitoring camera at the Kabuto Br.

(c) the water depth on the side walkways at the Shin-togagawa Br. estimated by video-taped images by a broadcast station

(d) the water surface pattern at the Kabuto Br. observed by the monitoring camera

Figure 12 presents comparison for the condition (a). The horizontal broken line indicates the measured data. The simulated water depth increases with the increase of input discharge. The irregular variation of roughness effect is due to the local variation of the bathymetry at the site. Figure 13 is the results for the condition (b). The horizontal shadowed zone is the estimated range of water depth. Figure 14 is the same expression for the condition (c).

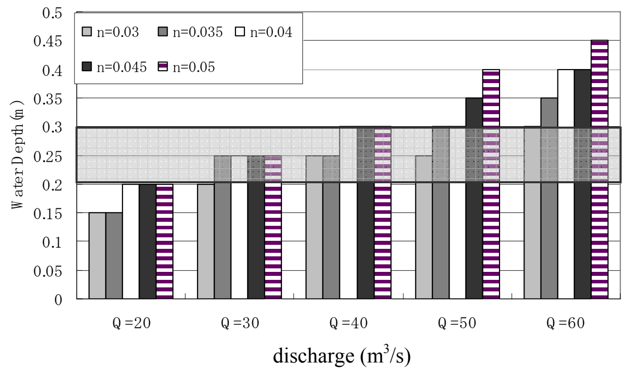

Figure 13. Comparison of water depth on side walkways at Kabuto Br.

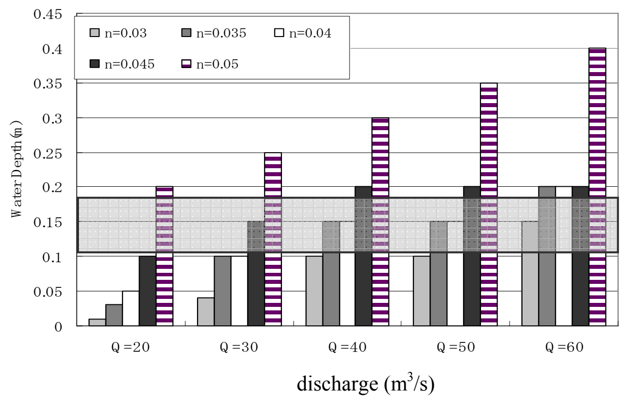

Figure 14. Comparison of water depth on side walkways at Shin-togagawa Br.

Although it is difficult to determine the only combination of the parameters satisfying all conditions, we concluded that the optimal combination is the maximum flow discharge of 40 cubic meters per second and the Manning's coefficient of 0.035. It should be noted that the peak discharge agrees with the roughly estimated value by the rational formula.

5 RESULTS AND DISCUSSIONS

5.1 *3D expression of the transient flash flood feature*

The simulated results of water surface patterns downstream of the Kabuto Br. at several time steps are demonstrated in Figure 15 in a form of 3D expression with an angle similar to the river monitoring camera. It is clearly seen that the flow is initially obstructed by the stepping stones in the lower channel. Then the elevated water gradually spreads upstream on the side walkways. However the backwater effect is restricted to a small region because most of flow region becomes supercritical as will be shown later in this chapter. The water surface displays significant undulation when the peak flow arrives at the section as shown in Figure 15(d). The simulated water surface configuration agrees fairly well with the image of the monitoring camera previously shown in Figure 6, except the side inflow from the drainage system. Figure 16 presents 3-D images from a viewing angle by a person left on the side walkway before and after the flash flood's arrival. Obviously the side walkways are fully covered by the water with considerable depth. The simulated results are presented by 3-D expressions from other viewing angles in a similar fashion to build animation movies, which will be distributed as an educational material for the people trying to utilize the water-friendly river environment in relatively small steep rivers.

5.2 *Flow pattern at peak flow*

Several hydraulic parameters in the channel downstream of the Kabuto Br. are provided in Figure 17 for the flow condition at the peak discharge together with a plan view of the site in normal condition. Figure 17(b) demonstrates that the water depth varies significantly from place to place with crossing shock waves just downstream of the bridge pier. It should be noted that local water depth becomes more than fifty centimetres even on the side walkways. Velocity distribution provided in Figure 17(c) shows that lower channel velocity becomes greater than five meters per second, while the velocity is still more than one meter per second even on the side walkways. It can be pointed out from Figure 17(d) that the Froude number distribution varies significantly from sub-critical to supercritical with the maximum value of about four.

In order to examine the force acting on the people at the time of the river accident, we calculated the distribution of hydrodynamic force from water depth and velocity distributions. The shape of the human body is assumed to be two cylinders when the flow depth is smaller than 0.5 meters and a larger cylinder for a deeper flow. The drag coefficient is assumed to be one in the calculation. The distribution of the hydrodynamic force thus calculated is shown in Figure 17(e). It is obvious that people on the side walkways are subjected to the local fluid force of more than 200N. This force level is almost equivalent to the force under which people are difficult to take even a step forward in the stream (Kunita et al., 2009).

6 CONCLUSIONS

The two dimensional simulation of the flash flood occurred in the Toga River due to torrential rain is conducted to reveal the cause of the water accident. It was made clear from the distribution of hydrodynamic force acting on human body in the river that people left on the side walkways must have been difficult to evacuate after the arrival of the flash flood because of the irresistible force acting on them. Therefore, an efficient alarming system for the flash flood is required for preventing those water accidents, occasionally have occurred in Japan in the past few years.

ACKNOWLEDGEMENTS

This research is financially supported by the foundation of River & Watershed Environment Management. Technical support by Dr. Tsubaki of Hiroshima University is greatly appreciated.

REFERENCES

Dekay, M. L., McClelland, G. H. 2006. Predicting loss of life in cases of dam failure and flash flood, Risk Analysis, 13(2), 193-205.

Fujita, I., Tsubaki, R. 2003. Evaluation of side concavity structure installed in urban river using finite volume method with unstructured grid system, 47, 523-528. (in Japanese)

Hoffman, K. A., Chiang, S. T. 1993. Computational Fluid Dynamics for Engineers, Vol.II, EES, 265-291.

Jonkman, S.N., Gelder, P.H.A.J.M.,Vrijling, J.K. 2002. Loss of life models for sea and river floods, Flood Defence 2002, Wu et al.(eds), 196-206.

Kunita, Y., Fujita, I., Ando, T. 2009. Estimation of discharge and flow feature at the time of water disaster in the Toga River caused by localized torrential rain. Advances in River Engineering, 15, 61-66. (in Japanese)

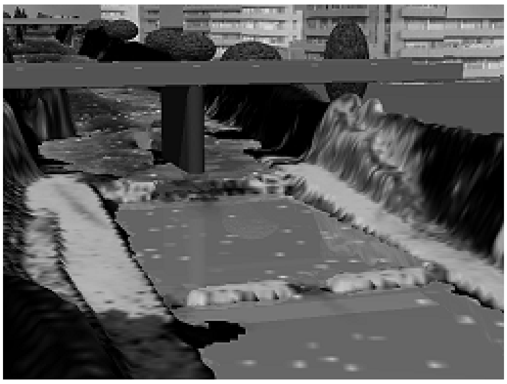

(a) flash flood just arrived

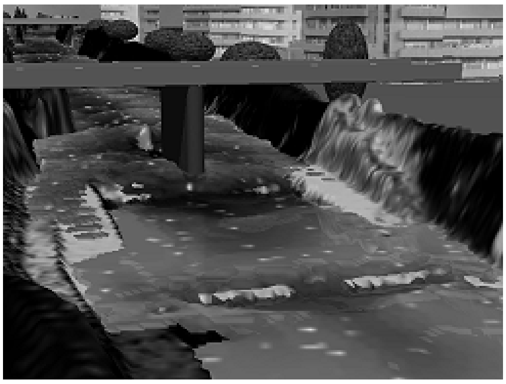

(c) flow obstructed by steps

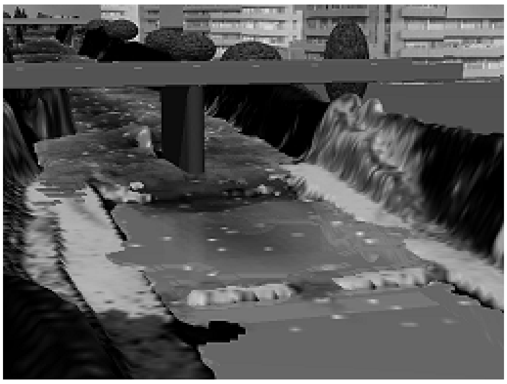

(b) lower channel overflow

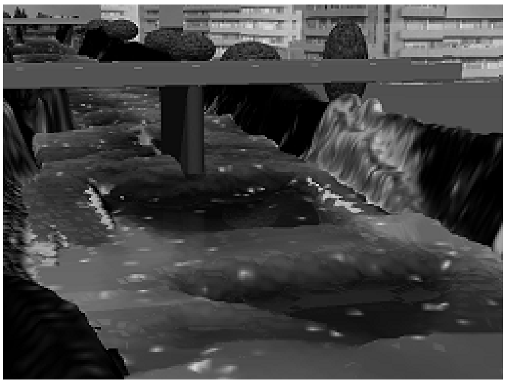

(d) flow undulates at peak dis-

Figure 15. Three-dimensional expression of simulated results near Kabuto Br.

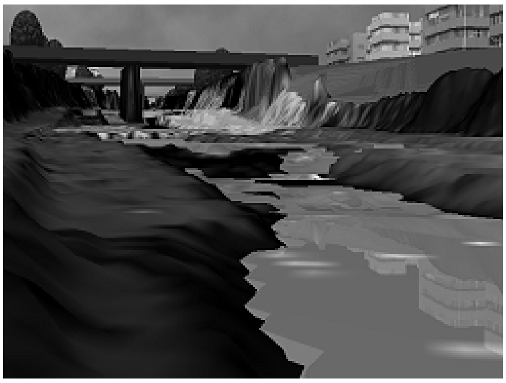

(a) before the arrival of flash

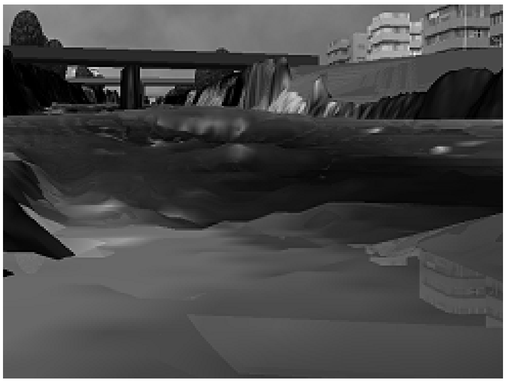

(b) at peak flow

Figure 16.Three-dimensional expression from a side walkway downstream of Kabuto Br.

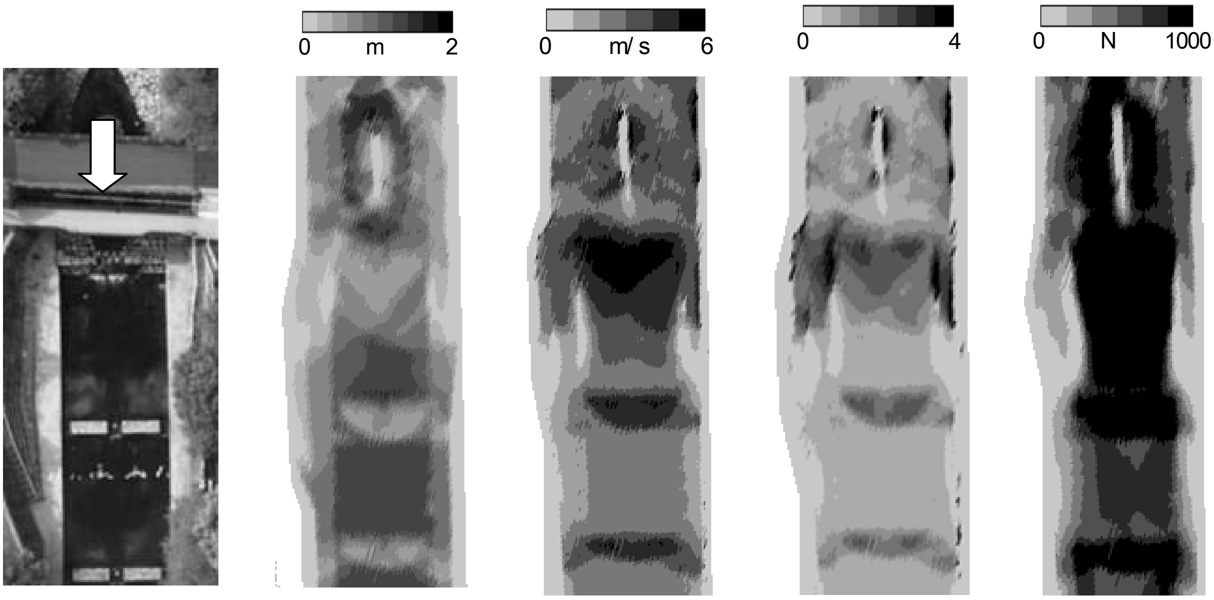

(a) plan view (b) water depth (c) velocity (d) Froude number (e) fluid force

Figure 17. Distribution of hydraulic parameters at Kabuto Br.